PERGAMON

Atmospheric Environment 36 (2002) 4635–4648

ATMOSPHERIC ENVIRONMENT

www.elsevier.com/locate/atmosenv

A replacement for simple back trajectory calculations in the interpretation of atmospheric trace substance measurements

Andreas Stohl[a,*], Sabine Eckhardt[a], Caroline Forster[a], Paul James[a], Nicole Spichtinger[a], Petra Seibert[b]

[a] *Department of Ecology, Technical University Munich, Am Hochanger 13, D-85354 Freising-Weihenstephan, Germany*
[b] *Institute of Meteorology and Physics, University of Agricultural Sciences, Türkenschanzstr. 18, 1180 Vienna, Austria*

Received 15 March 2002; received in revised form 2 June 2002; accepted 19 June 2002

Abstract

Trajectory calculations are often used for the interpretation of atmospheric trace substances measurements. However, two important effects are normally neglected or not considered systematically: first, measurements of trace substances sample finite volumes of air, whereas a trajectory tracks the path of an infinitesimally small particle; second, turbulence and convection. Advection by the deformative synoptic-scale atmospheric flow is responsible for the fact that a compact measurement volume is in fact turned into filamentary structures at earlier times, which a single trajectory cannot represent. Turbulence and convection add to this by causing a growth of the volume (backward in time) where processes such as emissions can affect measured concentrations. In this paper, we show that both effects are substantial and may be the largest sources of error when using trajectory calculations to establish source–receptor relationships. We use backward simulations with a Lagrangian particle dispersion model (LPDM) and cluster analysis of the particle positions to derive more representative single "trajectories" (transport paths) and trajectory ensembles. This reduces errors caused by filamentation and backward growth of the measurement volume to a few percent as compared to using a single, mean-wind trajectory and also yields estimates of the spread of the region of influence. Thus, we recommend to replace simple back trajectory calculations for interpretation of atmospheric trace substances measurements in the future by backward simulations with LPDMs, possibly followed by the clustering of particle positions as introduced in this paper.

Keywords: Pollution transport; Dispersion; Lagrangian particle dispersion model; Retroplumes, Source–receptor relationships

1. Introduction

Trajectories are, in meteorology, defined as the paths of infinitesimally small particles of air (Dutton, 1986). Such a fluid particle, 'marked' at a certain point in space at a given time, can be traced forward or backward in time along its trajectory. In practical trajectory models, this is done by integrating the trajectory equation $\Delta x_i = v_i \Delta t$ (where Δx is the position increment during a time step Δt resulting from the wind v; the index i runs from 1 to 3 and denotes the three dimensions of space), using mean (non-turbulent) horizontal and vertical winds from a meteorological model.

While forward trajectories describe where a particle will go, backward trajectories (often simply called back trajectories) indicate where it came from. Therefore, they are often used to interpret measurements of atmospheric trace substances, in order to establish relationships between their sources and their receptors (Stohl, 1998). Trajectory analysis is thus an essential element of practically all comprehensive air chemistry measurement campaigns (e.g., Fuelberg et al., 2001).

*Corresponding author. Tel.: +49-8161-71-4742; fax: +49-8161-71-4753.
E-mail address: stohl@forst.tu-muenchen.de (A. Stohl).

1352-2310/02/$ - see front matter
PII: S1352-2310(02)00416-8

Even large data sets are often investigated using back trajectories, allowing statistical analyses to be made (e.g., Ashbaugh, 1983; Moody and Galloway, 1988; Seibert et al., 1994; Stohl, 1996).

Trajectory calculations depend entirely on the input wind fields taken from a meteorological model, and thus inaccuracies in these data are the largest source of error for them (Stohl, 1998). Other sources of errors are the interpolation of the wind velocity from grid points to actual trajectory positions (Rolph and Draxler, 1990; Doty and Perkey, 1993; Stohl et al., 1995), and truncation errors which occur in the numerical solution of the trajectory equation (e.g., Walmsley and Mailhot, 1983; Seibert, 1993). Total trajectory position errors, resulting from all of the above sources together, are difficult to determine and are not normally known. A survey of results from previous studies employing different techniques suggests that average trajectory errors are on the order of 15–20% of the distance travelled after a few days (Stohl, 1998). However, in critical flow situations errors of up to 100% are also possible.

The quality of routinely available, gridded meteorological analyses has been improved substantially over the past decades, both in terms of accuracy and spatial resolution. Numerical schemes are accurate enough to render truncation errors negligible compared to other errors. Nevertheless, in many cases, calculated trajectories still fail to explain observed phenomena without clear reason. This paper shows that there are effects which are not or not well enough considered in trajectory calculation and interpretation procedures used for the analysis of measurement data, eventually leading to substantial errors in the source–receptor relationships inferred. An alternative procedure relying on a Lagrangian particle dispersion model (LPDM) has been developed and is presented here. The next section explains in detail the shortcomings of conventional methods and the outline of the alternative procedure. The latter is described in Section 3, a case study is presented in Section 4, and the results based on a large set of calculations are shown in Section 5. In the last two sections we discuss our results and draw conclusions.

2. The problem and outline of its solution

There are two reasons for problems when using back trajectories to interpret trace substance measurements. The first problem is that trajectories are the paths of infinitesimally small parcels (hereafter called particles) of air, whereas measurements require a finite and often large volume of air. This is true for remote sensing devices which require a finite backscatter volume as well as for in situ measurements which apply a certain collection or averaging time. Although, often used in practice, a single trajectory cannot normally be representative for the whole measurement volume.

Why is this so? Atmospheric flows are characterized by the presence of a kinematic property called deformation. In the two-dimensional case, this means that a circular fluid element will be torn into an elongated structure. Imagine, for example, such a fluid element arriving with a westerly flow at the border of a blocking high pressure system or a mountain range. The flow will then split into two branches going around the obstacle on either side. If the fluid element is on the dividing streamline, it will be torn apart into an elongated structure, eventually enclosing the whole obstacle, with separation of hundreds or thousands of kilometres. Repeated stretching and wrapping of fluid elements splits an initially compact volume of air into thin filaments during the course of time, which can be distributed over large areas and finally the whole atmosphere. As the atmospheric flows are three-dimensional, similar processes can happen in the vertical. This leads to even more effective separation as there is often substantial vertical wind shear, causing fluid elements at different levels to travel in different directions (Siems et al., 2000). The property of the atmosphere is thus that two particles which are initially close to each other will become separated by a large distance if sufficient time is allowed for; this is characteristic of a chaotic flow (Pudykiewicz and Koziol, 1998). These considerations hold for back trajectories as well, explaining why a single trajectory can be insufficient to represent the transport history of a sampling volume even if it is small.

Realizing these limitations, methods based on ensembles of trajectories were devised (e.g., Merrill et al., 1985; Kahl, 1993, 1996). Typically a few (often four) additional trajectories (sometimes called 'uncertainty' trajectories) are started at some distance from the measurement location, and their separation due to deformation in the wind field is used to estimate how representative the central trajectory is for each situation. These methods are insufficient because very few additional starting locations, selected more or less arbitrarily, are used, and because the effect of the finite sampling time is sometimes not taken into account. So there is no guarantee that the ensemble members are really representative of the whole volume of air sampled.

The second problem, which comes on top of the first one, is the presence of turbulent mixing and convection in the atmosphere. Near-ground measurements will by and large always take place in the atmospheric boundary layer (ABL) and thus in the presence of turbulence. It is well known that turbulence causes a puff of material released in the ABL to grow with time. The same is true for the volume of air which contributed to a short-term sampling, just with reversed direction (see Flesch et al. (1995), for a proof).

The combination of vertical turbulent diffusion and the vertical shear of the (horizontal) wind are especially important and are in fact the main reason for the horizontal dispersion in the mesoscale (Smith, 1965). There is some awareness that trajectories are therefore less accurate when they travel in the ABL or when they encounter deep convection. Crude attempts have been made to consider these effects in trajectory calculations (e.g., Stohl and Wotawa (1995), for boundary-layer transport, and Freitas et al. (2000), for convective transport), but they are not going far enough, because trajectories calculated with the mean wind fields cannot represent this mixing process and the growth of the volume of influence. In addition to being a mechanism of its own, this growth also enables deformation processes to become more effective, because the volume they can act upon grows—initially rapidly—with time.

Nowadays, we have sufficient computer capacities for more accurate solutions of both problems. The requirement of these solutions is that they can track a volume of air forward or backward in time under the effects of turbulent mixing, of convection, and of the three-dimensional structure of atmospheric flows including deformation. This is the task of a transport and dispersion model for forward tracking and of its adjoint for backward tracking. One class of such models are LPDM (Thomson, 1987; Rodean, 1996). They are especially well suited for our task as they are an extension of the simple trajectory models, are capable of representing transport processes with strong filamentation in a very accurate way, and can handle 'point' measurement sites without artificial diffusion such as present in Eulerian (grid) models. LPDMs account for turbulence in a stochastic way by calculating the trajectories of a large number of particles transported by both the mean wind and statistically modelled turbulent fluctuations (Rodean, 1996). They can also be run backward in time (e.g., Flesch et al., 1995; Seibert, 2001).

However, the interpretation of LPDM output in backward mode is not as straightforward as in the normal forward mode. The simplest interpretation is to consider the LPDM as a tool to calculate back trajectories determined not only by the mean wind but also by turbulent motions. As turbulence is stochastic, it is not possible anymore to be sure that such a trajectory represents the path of a real air particle, but a sufficiently large ensemble of trajectories should correctly represent the behaviour of the ensemble of real air particles. In analogy to forward calculations, we may call the cloud of tracer particles a retroplume. Using a LPDM, thus, quantitative source–receptor relationships can be calculated (Seibert and Stohl, 2000; Seibert, 2001).

Now, when it is clear that LPDMs are physically more correct than trajectory models, why are the latter still used? There are different answers to this question (e.g., convenience, availability of models, computational constraints), but most important is the overwhelming complexity of the LPDM output compared to a simple trajectory. The LPDM output is four-dimensional, whereas back trajectories are quasi-one-dimensional. Back trajectories can be represented on a map with a simple line (color-code for the height, markers for time), while a corresponding LPDM output, if visualized in the same way, would consist of several thousands of such lines (or, alternatively, of gridded four-dimensional fields), and thus be unreadable. For a large data set, consisting of several thousands of individual measurements, the difficulties multiply, because many of the established techniques for statistical trajectory analysis cannot be used with LPDM output, due to computational or other constraints. Finally, trajectory data are more easy to share between modelers and experimentalists.

The aim of this paper is therefore to make best use of both methods: LPDM and trajectory calculations. We have developed a technique that reduces the results of a LPDM simulation to the equivalent of a few back trajectories, which are more accessible to subsequent analysis than the full LPDM output, but preserve as much information as possible.

3. Description of the new method

For our studies we use the LPDM FLEXPART version 4.3 (Stohl et al., 1998) which was used in several studies of long-range transport of trace substances (e.g., Stohl and Trickl, 1999; Forster et al., 2001). It can also be run in backward mode (Seibert, 2001). In the applications shown here, FLEXPART was used with global meteorological input fields from the European Centre for Medium-Range Weather Forecasts (ECMWF, 1995) with a horizontal resolution of 1°, at all the 60 vertical model levels, and with a time resolution of 3 h (analyses at 0, 6, 12, 18 UTC; 3-h forecasts at 3, 9, 15, 21 UTC). FLEXPART treats advection and turbulent dispersion by calculating the trajectories of a multitude of particles. Solving Langevin equations, stochastic fluctuations of the three wind components are superimposed on the grid-scale winds to represent transport by turbulent eddies (Stohl and Thomson, 1999). To represent convective transport, FLEXPART was recently equipped with the convection scheme developed by Emanuel and Zivkovic-Rothman (1999). Its implementation is described in Seibert et al. (2001).

In each LPDM run we calculate the trajectories of 2000 particles and use their position data for deriving a condensed model output. The first output parameter is called the retroplume centroid (RPC, see also Table 1),

Table 1
Characterization of the different trajectory types used

Abbreviation	Name	Turbulence	Initial location in volume	No. of particles	No. of clusters
RPC	Retroplume centroid	Yes	Domain-filling	2000	1
RPCC	Retroplume cluster centroids	Yes	Domain-filling	2000	5
NT-CL	Non-turbulent central-location	No	Central	1	1
NT-RL	Non-turbulent random-location	No	Random	1	1
T-CL	Turbulent central-location	Yes	Central	1	1
T-RL	Turbulent random-location	Yes	Random	1	1

defined as the centroid of all particles at a given time. The sequence of these RPC positions is the more representative correspondence to a conventional trajectory. Be aware, though, that the RPC can lie outside the retroplume if its structure is concave or if it is split into several parts. For forward dispersion, plume centroid trajectories have been used previously in the context of large-scale tracer experiments (e.g., Draxler, 1987; Haagenson et al., 1990).

Next, we perform on-line cluster analyses of the particle positions at selectable time intervals. Cluster analysis is a semi-objective method (Kalkstein et al., 1987) applied here to determine a few locations that best characterize the position and shape of the entire retroplume. It is thus a way of reducing the enormous output of a LPDM as much as possible while maintaining the maximum required information. The clusters are similar to ensemble trajectories, but are more objective and less arbitrary. The cluster analysis minimizes the root-mean-square distance (RMSD) between the particles of each of the clusters and their respective retroplume cluster centroids (RPCC), and maximizes the RMSD between the RPCC. The number of particles belonging to each of the clusters can be different and depends on the retroplume's shape. We expect that with the clustering the total RMSD will be significantly reduced compared to the RPC trajectory (which is equivalent to a single cluster only). As the clustering is performed independently each time, subsequent RPCC do not lie on a trajectory and thus cannot be connected by a line in a trajectory plot. The clustering is applied to the horizontal trajectory positions and thus aims at reducing RMSD in the horizontal, but vertical RMSD are also reduced as a by-product. The number of clusters is fixed at 5 here as this provides an acceptably small amount of data for subsequent analyses.

To determine the difference to traditional trajectory calculations, we carry four additional flagged particles in the LPDM simulation. One pair of particles is released exactly at the center of the sampled air, and the other pair is initialized from random locations within the sampled volume. For two of the particles (one from each pair) turbulence is switched off, whereas for the other two (again, one from each pair) it is turned on. The non-turbulent central location (NT-CL, see Table 1) trajectory is a simple back trajectory starting at the "ideal" position, whereas the non-turbulent random-location (NT-RL) trajectory is a simple trajectory started somewhere in the measurement volume. The turbulent central-location (T-CL) trajectory is started at the "ideal" position, and the turbulent random-location (T-RL) trajectory resembles an arbitrarily selected member of the ensemble of 2000 retroplume trajectories. As a measure of deviation we use the RMSD between a trajectory's position and the 2000 retroplume particle positions. Our comparisons are idealized in the sense that we assume that the calculated retroplumes are exact. Thus, we study effects resulting from retroplume growth and deformation only and ignore other possible errors, such as wind field errors.

Two series of backward simulations, representing typical tasks for a trajectory model, are performed. First, think of tropospheric lidar measurements to be interpreted with trajectories. Typically, such data would be presented as a vertical profile with 500 m vertical and 30 min temporal resolution. Thus, in the first example we release 2000 particles, continuously distributed between 5000 and 5500 m and over a time interval of 30 min (furtheron referred to as the mid-tropospheric sampling case). For the second example think of in situ trace gas measurements made at the ground. These data also have a typical time resolution of 30 min. Thus, within 30 min we release 2000 particles equally distributed between the surface and 100 m a.s.l. Particles are quickly mixed over the entire depth of the ABL and thus a lower release height would make little difference for the turbulent trajectories. However, the non-turbulent trajectories would be initialized at unreasonably low altitudes, leading to very large RMSD because of the vertical shear of the horizontal wind.

4. A case study

Fig. 1 shows, as an example, backward LPDM calculations for an air volume arriving between 5000 and 5500 m a.s.l at the position of Mace Head, Ireland (51.6°N, 11.5°W), on 30 December 2000 between 11:45

and 12:15 UTC. The model calculation is done 10 days backward in time and model output is generated every 3 h. The quantity shown indicates the strength of the signal which would be produced at the receptor by a source located on the map. In addition, Fig. 1 shows, overlaid over the retroplume, the trajectories of the four flagged particles, the RPC trajectory, and the RPCC positions. During the first 3 days, the retroplume is compact and all trajectories remain together closely. After 3 days, when the retroplume starts to circle around a high-pressure system, the trajectories begin to fork. After 5.5 days (Fig. 1, top), the main part of the retroplume is still compact, but a filament has been sheared off and travels southeastwards (back in time). None of the flagged particle trajectories traces this part of the retroplume. The RPC trajectory reflects the filament's presence by its southeastward shift from the retroplume's main part. The cluster analysis successfully characterizes the retroplume's shape. Three RPCC, which together represent 76% of the particles, are spread over the main part of the retroplume, one RPCC is found in the middle, and one at the end of the filament. Note also that the 3 large RPCC are positioned at an altitude of approximately 8000 m, while the filament's tip is below 5000 m.

As it loops around the high 6.5 days back, the retroplume becomes dispersed over some 80° of longitude (Fig. 1, middle). The filament between Iceland and Great Britain is now cut off entirely from the retroplume's main part. One of the non-turbulent trajectories traces the center of the retroplume, whereas the other loops around the high to the far end of the retroplume. Obviously, if only one of them were available, misleading conclusions on the "origin" of the air mass could be drawn, placing it either over Canada or Greenland. The cluster analysis is more successful in characterizing air mass origin.

Ten days back, particles are found almost throughout the mid-latitude North Atlantic (Fig. 1, bottom). The RPC trajectory is placed close to the particle density maximum, but the four flagged trajectories all end in the southeastern part of the retroplume, one even at its end. The cluster analysis places the three largest RPCC along the main retroplume filament, a smaller one southwest of Greenland, and a very small one within the tracer parcel over New England. The RPCC southwest of Greenland is at an altitude of about 8000 m, whereas the other RPCC are between 1500 and 4500 m.

In this example, cluster analysis of particle positions is more successful in characterizing the retroplume than any single back trajectory or even the four flagged trajectories together. This example was not chosen because the retroplume is more complex than in other cases. Rather the opposite is true: The RMSD of the RPC trajectory after 10 days is 1400 km, less than half of the 1-yr average (see Section 5). Thus, in other cases single trajectories will fail even earlier than in our example to characterize the retroplume. It is also clear that, even using cluster analysis, a lot of information will be lost after 10 days.

5. Statistical results

To have a data set suitably large for statistical analysis, we repeat the simulations twice a day for the year 2000, yielding a total of 730 cases for each of the assumed surface and mid-tropospheric sampling series. Even though calculations were done only for Mace Head and results likely would be somewhat different for other geographical locations, this will not affect our general conclusions. For the mid-tropospheric sampling, three different model calculations were carried out, namely with both turbulence and convection parameterizations turned off (NT + NC), with turbulence parameterizations only (T + NC), and with both turbulence and convection parameterizations turned on (T + C). This allows to study the effects of advection alone (which leads only to filamentation and not to retroplume growth), plus the additional effects of turbulence and convection. For the surface sampling, only the results for the T + NC case are presented, as in this case ABL turbulence is most important.

Fig. 2 shows the results for the NT + NC (i.e., pure advection) midtropospheric sampling case. In the figure, the average RMSD between the 2000 retroplume particle positions and the trajectory positions for the trajectory types NT-CL, NT-RL, RPC and RPCC are plotted as a function of time. Note that because turbulence was switched off, the T-CL and T-RL trajectories were not available in this case. Both horizontal and vertical RMSD are shown, and horizontal RMSD are expressed in both absolute and relative terms. Relative units were obtained by dividing RMSD with the average length (i.e., the sum of the lengths of the 3 h segments) of the NT-CL trajectories. After 10 days the RPC trajectories are, on average, about 20% shorter than the NT-CL trajectories, because their path is smoother than the NT-CL trajectories' path. Thus, if RMSD were divided by the average RPC trajectories' length, relative values were about 20% larger. Relative RMSD decrease during the first few hours of transport before increasing again. The initial decrease is an artifact of the half-hour duration of the particle release. Time is counted from the middle of the sampling interval, when the retroplume already has grown to a certain size, but the NT-CL trajectory has not yet started travelling.

RMSD grows backward in time for all trajectory types (Fig. 2). RMSD growth is slow, but accelerating, in the first 4 days or so. After about 4 days, RMSD growth is approximately linear with time, in agreement

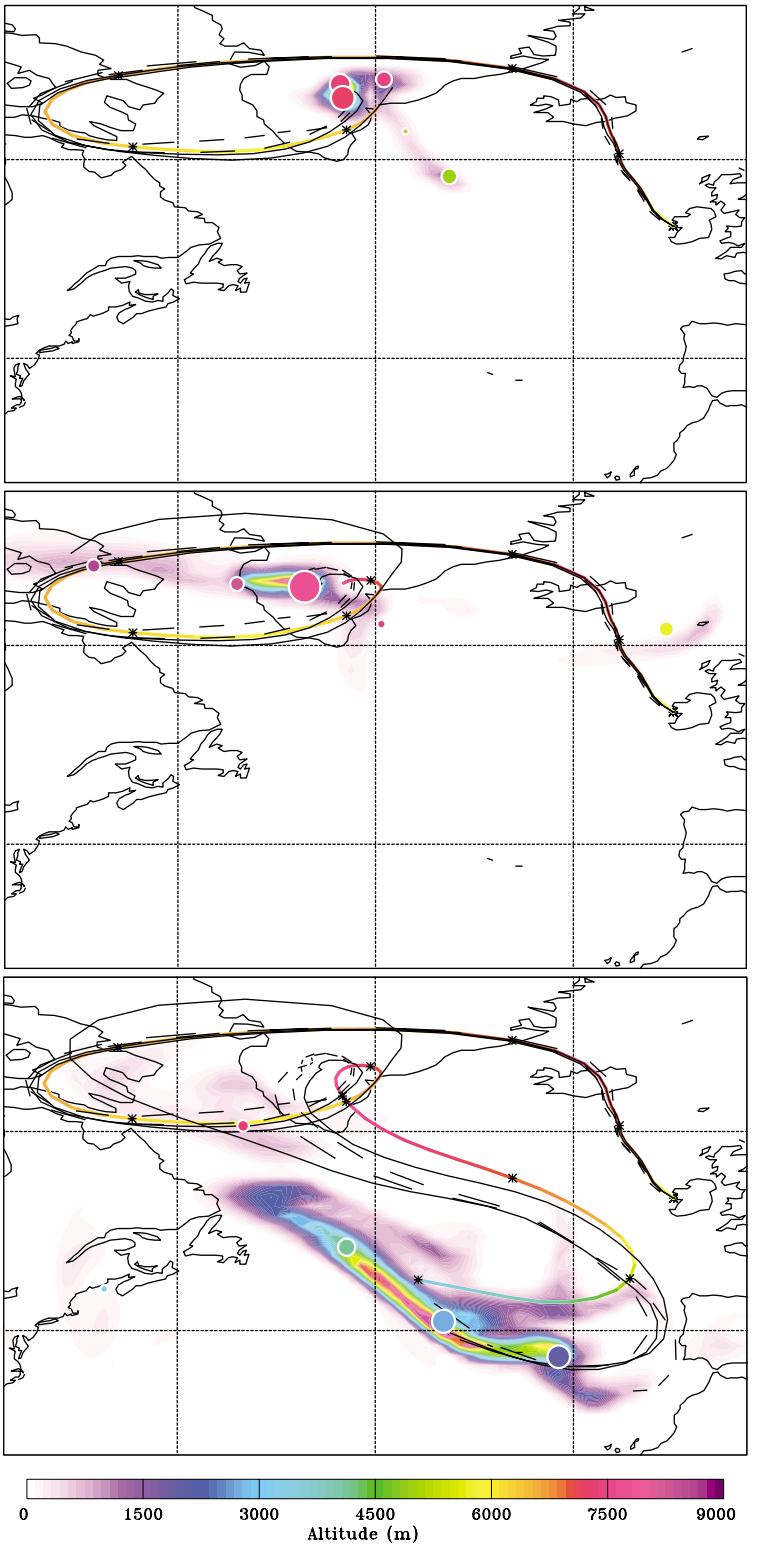
0
1500
3000
4500
6000
7500
9000
Altitude (m)

with the theory of long-range atmospheric dispersion (Arya, 1999). After 10 days, both NT-CL and NT-RL trajectories have very large RMSD of about 3200 km or 23% of the travel distance, which is comparable to, or even larger than, typical trajectory errors resulting from all sources of error together (Stohl, 1998). During the first few days (best seen in the relative RMSD plots, Fig. 2, middle panel) the differences between the two flagged trajectories are relatively large, with the NT-CL trajectories travelling closer to the RPC. However, after 10 days both have similar RMSD, indicating that accuracy is not much improved by starting the trajectories exactly at the center of the volume.

Tracing the RPC instead of an individual particle, reduces the RMSD significantly. But after 10 days RMSD is still 2500 km or about 17% of the transport distance, which is still on the same order of magnitude as typical trajectory errors. Only the cluster analysis can reduce RMSD to values smaller than typical trajectory errors. After 10 days, RMSD for the RPCC trajectories is about 800 km, or just above 5%. During the first 4 days it is even below 2%, which is an order of magnitude smaller than typical trajectory errors. Note that the clustering actually can decrease RMSD to any desired level, if the number of clusters is increased. But even with only 5 RPCC, the RMSD reduction is substantial.

Vertical RMSD are also very large (almost 3000 m for the NT-CL and NT-RL trajectories after 10 days), but show similar characteristics as horizontal RMSD. Although the clustering was done with respect to the horizontal positions, it is also quite successful in reducing vertical RMSD (by more than 50% relative to the NT-CL and NT-RL trajectories). The reason for that is that parts of the particle cloud at different levels will be transported by winds with different directions and velocities, like in the case study shown above.

Fig. 3 shows the same as Fig. 2, but with turbulence switched on. After 10 days, RMSD of the individual trajectories are almost 4000 km or about 27% of the travelled distance. Differences between all 4 flagged-particle trajectories are rather small. Both non-turbulent trajectories have somewhat smaller RMSD than the turbulent ones, as they tend to trace the RPC more closely. The RMSD reduction by the RPC is again significant, but not large enough to yield acceptable results. The amount of reduction of the RMSD achieved by considering the five clusters indicates that the total spread of the particle cloud is well captured with this number of clusters and reduces the RMSD to values below typical trajectory errors.

Switching on also the convection parameterization further increases RMSD of all trajectory types (not shown). The individual trajectories now have RMSD of 4100–4300 km (i.e., relative RMSD of more than 30%) after 10 days, RPC trajectories have a mean RMSD of 3300 km (24%), and RPCC trajectories have a mean RMSD of about 1300 km (9%). Vertical RMSD are also substantially increased compared to the convection-free cases: 3600 m for individual trajectories, 2600 m for RPC trajectories, and 2200 m for RPCC trajectories, after 10 days.

For the ABL sampling the largest RMSD are produced by the non-turbulent trajectories (Fig. 4), which is different from the mid-tropospheric sampling cases. The reason for this is that the non-turbulent trajectories neglect the vertical mixing within the ABL. This is accounted for by the turbulent trajectories, whereas the altitude of the non-turbulent trajectories can increase only due to the grid-scale vertical motion. RMSD could possibly be reduced by starting the non-turbulent trajectories at a higher altitude. For instance, 925 or 850 hPa are often used as starting heights for back trajectories from surface stations. However, because ABL heights vary both seasonally and with the time of the day, a constant starting altitude is not a real solution.

Absolute RMSD are comparable to the mid-tropospheric sampling case, but, because of the lower wind speeds in the lower troposphere, the relative RMSD are much larger, on the order of 40% of the distance travelled after 10 days. Again, only the clustering can reduce RMSD to an acceptable level. However, vertical RMSD are quite large, even after clustering.

Fig. 1. Maps showing the retroplume starting from an altitude range 5000–5500 m a.s.l. over Mace Head on 30 December 2000 between 11:45 and 12:15 UTC. Depicted on the map, which covers the Atlantic region (77°W–3°W, 28°N–75°N), are vertically averaged particle densities 5.5 days back (top), 6.5 days back (middle) and 10 days back (bottom), colored according to the particle density in arbitrary units. Superimposed on the retroplume are; (1) the RPC trajectory (thick line colored according to altitude as given in the label bar; positions are marked with asterisks every 24 hours); (2) the NT-CL trajectory starting at 5250 m a.s.l. at 12 UTC, and the NT-RL starting at an arbitrary location in space and time within the assumed altitude range and time interval (both in solid black lines); (3) the T-CL trajectory starting at 5250 m a.s.l. at 12 UTC, and the T-RL trajectory starting at an arbitrary location in space and time within the assumed altitude range and time interval (both dashed black lines); and (4) the five RPCC positions (dots colored according to altitude as given in the label bar; the dots' size is scaled with the number of cluster members). RPCC positions are shown only for the times for which retroplumes are also shown, whereas trajectories are drawn from the starting position to the time for which the retroplume is shown. Note that the same color code is used both for the RPCC vertical positions and for the retroplume's particle density.

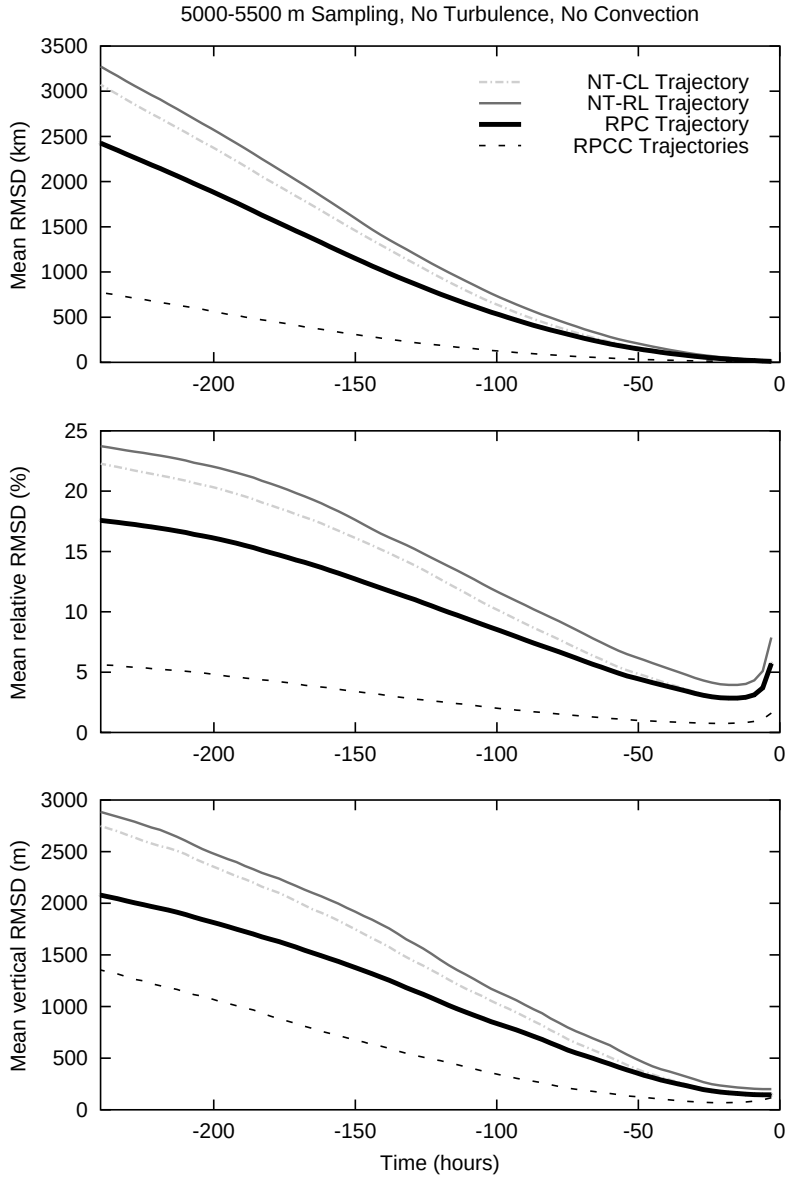

Fig. 2. RMSD, averaged over the results of 730 FLEXPART simulations, as a function of time backward from the middle of the assumed 30-min sampling interval, for the NT + NC (i.e., pure advection) mid-tropospheric sampling case. Results are shown for the trajectory types NT-CL (dash-dotted grey line), NT-RL (solid dark grey line), RPC (thick solid black line) and RPCC (dashed black line), and for absolute horizontal RMSD (top), relative horizontal RMSD (middle), and vertical RMSD (bottom).

6. Discussion

We have studied two series of reverse LPDM calculations. In both the series it was assumed that the air was sampled for half an hour, and that a certain vertical resolution applies. Large RMSD of single trajectories from the plume particles were found which are greater than typical trajectory errors. Certainly, for smaller sample volumes, smaller retroplumes and thus smaller RMSD would have been obtained. However, many measurements sample larger, rather than smaller, volumes than we have used. Furthermore, especially in the ABL turbulence makes a small retroplume grow rapidly and thus the sampling volume is less important than the magnitude of turbulence encountered and variations in ABL height. Neglecting initial sampling

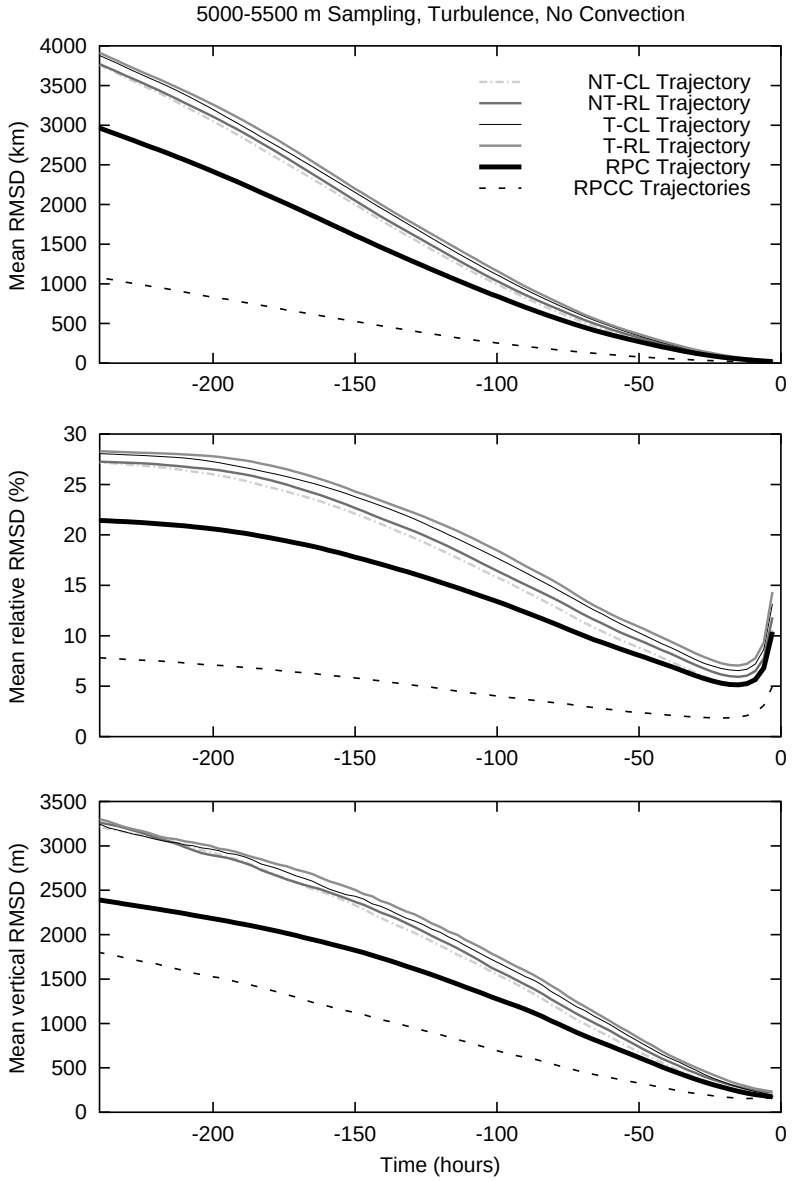

Fig. 3. RMSD, averaged over the results of 730 FLEXPART simulations, as a function of time backward from the middle of the assumed 30-min sampling interval, for the T + NC (i.e., turbulence only) mid-tropospheric sampling case. Results are shown for the trajectory types NT-CL (dash-dotted grey line), NT-RL (solid dark grey line), T-CL (thin solid black line), T-RL (dotted grey line) RPC (thick solid black line) and RPCC (dashed black line), and for absolute horizontal RMSD (top), relative horizontal RMSD (middle), and vertical RMSD (bottom).

volumes and/or turbulence thus can always cause serious errors in derived source–receptor relationships for the sample.

LPDM results depend on parameterizations of turbulence and convection, which are less accurate than the winds resolved by the meteorological analyses. Thus, replacing a trajectory model with a LPDM introduces a significant additional source of error. However, even larger errors in source–receptor relationships based on traditional trajectory calculations occur by ignoring turbulence and convection. While it is of course desirable to improve the parameterizations, we firmly believe that even with those currently available trajectory accuracy can be improved.

A critical factor for the applicability of the RPCC method is computation time. As implemented in

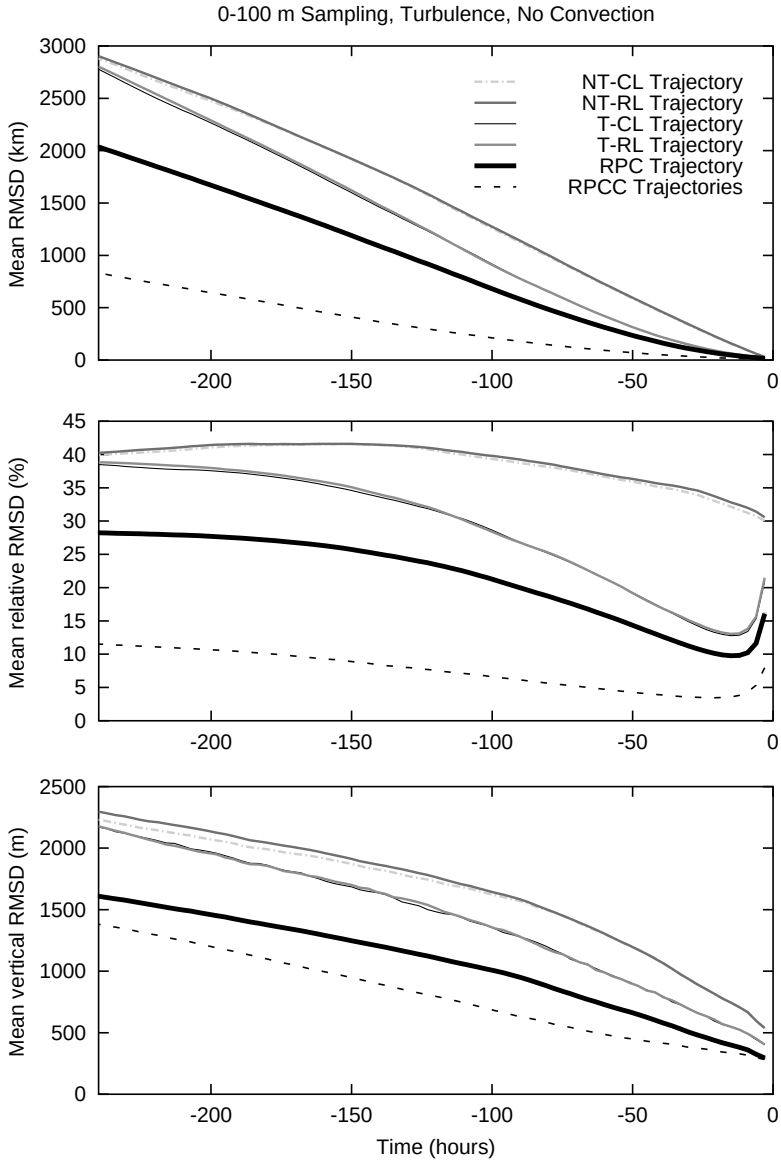

Fig. 4. Same as Fig. 3, but for the surface sampling T + NC case.

FLEXPART, the CPU time for 730 individual 10-day backward simulations (i.e., two per day over a 1-yr period) with 2000 particles each and without convection parameterization was about 45 h on a Linux workstation with a 1 GHz Pentium III processor. This appears acceptable given the tremendous gain in accuracy compared to traditional trajectory calculations. Furthermore, there is potential for further optimizations. For example, the number of particles could be reduced to a few hundred per simulation without large loss of information, especially for shorter travel times, and the cluster analysis, which is rather time-consuming, could be stopped before perfect convergence is achieved.

We receive additional benefits from the LPDM simulation compared to normal trajectory calculations. For instance, often it is important to know to what extent a sampled air volume was influenced by air from the boundary layer or by air from the stratosphere. At every time step we thus calculate the fraction of particles that reside inside the ABL, the fraction located above the thermal tropopause, and the fraction with a potential vorticity greater than a threshold value considered to be representative for the stratosphere.

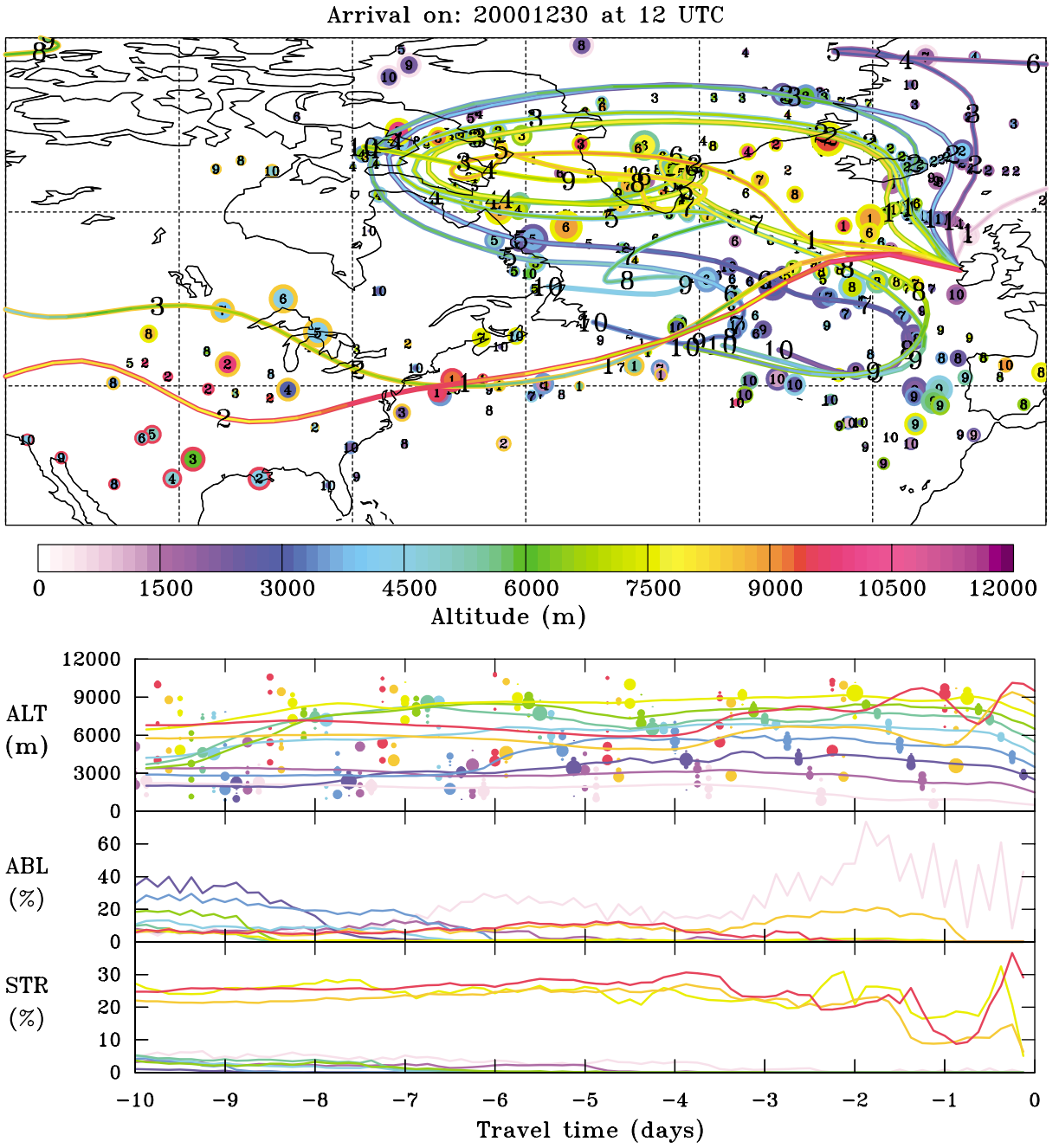

Fig. 5. Characterization of ten "retroplumes" for a hypothetical vertical sounding from 0 to 10000 m with a resolution of 1000 m at the location of Mace Head on 30 December 2000 at 12 UTC. In the upper map, RPC trajectories are drawn for each of the 10 height intervals. Each trajectory consists of a middle line, the color of which (according to the label bar) indicates the actual trajectory height, that is framed by two outer lines of constant color representing arrival height. Time backward in days is indicated by large numbers along the RPC trajectories. In addition, the RPCC positions are plotted as dots every 24 hours. The dots' size is scaled with the number of cluster members, the inner dots' color codes for actual RPCC height, and the outer dots' color codes for arrival height. Numbers on the dots give the days backward in time. The lower panels show timeseries of the altitudes of the RPC trajectories (lines) and, every 30 h, the heights of the RPCCs (dots whose size scales with the number of cluster members) (coloring for both lines and dots according to arrival height); the fraction of the particles residing in the ABL; and the fraction of particles residing in the stratosphere (coloring again according to arrival height).

This preserves important information from the full LPDM simulation. And finally, the RMSD values are calculated totally and for each cluster individually. As the RMSD varies substantially from case to case, this is an important information on the representativity. There is also the option of regular backward LPDM simulations using gridded output of full quantitative source–receptor relations, which certainly is the method of choice if only a limited number of observations are to be interpreted and thus the LPDM output remains manageable.

Graphical presentation of the results of our new method is somewhat different from traditional trajectory (or trajectory ensemble) plots and is considerably more complex. Fig. 5 shows, for the same case as described in Section 4, one possibility of how the results of several calculations can be visualized in one plot. For the plot it was assumed that an atmospheric sounding upto 10 km with a vertical resolution of 1 km was made. For each altitude interval, a LPDM backward calculation was performed and characterized by the RPC trajectory and the RPCCs. Detailed information on the origin of the air masses at different levels is contained in the chart. For instance, the altitudes at which the different air masses travelled and the geographical regions from where they originated can be clearly distinguished. It is also readily seen to which extent each measurement was influenced by air from the stratosphere and the ABL. With our method, the major transport processes influencing an entire atmospheric sounding can thus still be visualized in a single, admittedly complex, plot. Once acquainted with these charts, a series of them could, for instance, be used to efficiently investigate the nature of all the structures typically seen in lidar timeseries.

We conclude this section with a cautionary note on the terms accuracy and uncertainty. By definition, RMSD obtained for a set of RPCC will be smaller than the RPC RMSD, which in turn will be smaller than any single trajectory's RMSD. Thus, the retroplume structure is always best characterized by the set of RPCC and, hence, we consider our method as more accurate. However, when a pollution source shall be identified this is a small advantage in cases when the retroplume covers the whole (or large parts of the) atmosphere, because then the source can be located everywhere, and the method does not help to determine the origin of the pollutant. The nature of dispersion leads to a loss of information (equivalent to an increase of entropy) with time. Therefore, the scale of potential source regions for which meaningful information can be obtained becomes larger the longer we go back in time, irrespective of what method we use for the calculations. However, our method yields at least an estimate of this scale, in contrast to single back trajectory calculations.

7. Conclusions

Single back trajectory calculations neglect that trace substance measurements in the atmosphere require a certain volume of air to be sampled. Advection in chaotic flows leads to filamentation of this volume of air, which cannot be represented by a single trajectory. Furthermore, turbulence increases the volume of air from where influences (emissions, for example) can be propagated into the measurement. We have quantified the errors that are incurred if these effects are neglected, and we have developed a method to take them into account properly while still producing a well-manageable output, based on LPDM simulations and output condensation by cluster analysis. Our conclusions are summarized as follows:

- The average RMS deviations due to retroplume filamentation and growth between individual trajectories and the condensed LPDM output are on the order of 20–40% of the distance travelled after 10 days. This is more than the errors resulting from wind field analysis, interpolation and numerical truncation together. It is thus of vital importance to consider retroplume growth and filamentation in receptor-oriented transport simulations for the interpretation of atmospheric trace substance measurements.
- Tracing the retroplume's centers yields an ensemble-average trajectory that is more representative than any single-particle trajectory. After 10 days, the average RMSD of the ensemble- average trajectories is approximately 20–30% smaller than that of the individual trajectories. However, this is still large compared to other trajectory errors.
- LPDM output is four dimensional and thus quite big and complex. Therefore, in order to analyze large measurement data sets, a way had to be developed to condense the enormous LPDM output into a workable data set. We propose cluster analysis of particle positions for this purpose, as it preserves a maximum of information in a minimum of output.
- Using five clusters, which leads to data sets comparable in size to current ensemble-trajectory methods, about 90% of the spread of the cloud is still being captured for 10-day backward simulations.
- Thus we recommend to replace simple back trajectory calculations for the interpretation of atmospheric trace substance measurements by backward simulations with a LPDM, possibly combined with on-line clustering of particle positions as introduced here.

The source code and documentation of FLEXPART can be downloaded from http://www.forst.tu-muenchen.de/EXT/LST/METEO/stohl/.

Acknowledgements

This study was part of the projects CARLOTTA, ATMOFAST and CONTRACE, funded by the German Federal Ministry for Education and Research within the Atmospheric Research Program 2000 (AFO, 2000). We thank K. Emanuel for making available the source code of the convection scheme, and A. Frank for assistance in implementing it into FLEXPART. ECMWF and the German Weather Service are acknowledged for permitting access to the ECMWF archives. Two anonymous referees are acknowledged for careful reading. Their thoughtful reviews helped to improve this manuscript.

References

Arya, S.P., 1999. Air Pollution Meteorology and Dispersion. Oxford University Press, New York.

Ashbaugh, L.L., 1983. A statistical trajectory technique for determining air pollution source regions. Journal of Air Pollution Control Association 33, 1096–1098.

Doty, K.G., Perkey, D.J., 1993. Sensitivity of trajectory calculations to the temporal frequency of wind data. Monthly Weather Review 121, 387–401.

Draxler, R.R., 1987. Sensitivity of a trajectory model to the spatial and temporal resolution of the meteorological data during CAPTEX. Journal of Climate and Applied Meteorology 26, 1577–1588.

Dutton, J.A., 1986. The Ceaseless Wind an Introduction to the Theory of Atmospheric Motion. Dover, New York, 617pp.

ECMWF, 1995. User Guide to ECMWF Products 2.1. Meteorological Bulletin M3.2. ECMWF, Reading, UK.

Emanuel, K.A., Zivkovic-Rothman, M., 1999. Development and evaluation of a convection scheme for use in climate models. Journal of Atmospheric Science 56, 1766–1782.

Flesch, T.K., Wilson, J.D., Yee, E., 1995. Backward-time Lagrangian stochastic dispersion models and their application to estimate gaseous emissions. Journal of Applied Meteorology 34, 1320–1332.

Forster, C., Wandinger, U., Wotawa, G., James, P., Mattis, I., Althausen, D., Simmonds, P., O'Doherty, S., Kleefeld, C., Jennings, S.G., Schneider, J., Trickl, T., Kreipl, S., Jäger, H., Stohl, A., 2001. Transport of boreal forest fire emissions from Canada to Europe. Journal of Geophysics Research 106, 22887–22906.

Freitas, S.R., et al., 2000. A convective kinematic trajectory technique for low-resolution atmospheric models. Journal of Geophysical Research 105, 24375–24386.

Fuelberg, H.E., et al., 2001. A meteorological overview of the second Pacific Exploratory Mission in the Tropics. Journal of Geophysical Research 106, 32427–32443.

Haagenson, P.L., Gao, K., Kuo, Y.-H., 1990. Evaluation of meteorological analyses, simulations, and long-range transport using ANATEX surface tracer data. Journal of Applied Meteorology 29, 1268–1283.

Kahl, J.D., 1993. A cautionary note on the use of air trajectories in interpreting atmospheric chemistry measurements. Atmospheric Environment 27A, 3037–3038.

Kahl, J.D.W., 1996. On the prediction of trajectory model error. Atmospheric Environment 30, 2945–2957.

Kalkstein, L.S., Tan, G., Skindlov, J.A., 1987. An evaluation of three clustering procedures for use in synoptic climatological classification. Journal of Climate and Applied Meteorology 26, 717–730.

Merrill, J.T., Bleck, R., Avila, L., 1985. Modeling atmospheric transport to the Marshall islands. Journal of Geophysical Research 90, 12927–12936.

Moody, J.L., Galloway, J.N., 1988. Quantifying the relationship between atmospheric transport and the chemical composition of precipitation on Bermuda. Tellus 40B, 463–479.

Pudykiewicz, J.A., Koziol, A.S., 1998. An application of the theory of kinematics of mixing to the study of tropospheric dispersion. Atmospheric Environment 32, 4227–4244.

Rodean, H., 1996. Stochastic Lagrangian models of turbulent diffusion. Meteorological Monographs, Vol. 26(48). American Meteorological Society, Boston, USA.

Rolph, G.D., Draxler, R.R., 1990. Sensitivity of three-dimensional trajectories to the spatial and temporal densities of the wind field. Journal of Applied Meteorology 29, 1043–1054.

Seibert, P., 1993. Convergence and accuracy of numerical methods for trajectory calculations. Journal of Applied Meteorology 32, 558–566.

Seibert, P., 2001. Inverse modelling with a Lagrangian particle dispersion model: application to point releases over limited time intervals. In: Gryning, S.E., Schiermeier, F.A. (Eds.), Air Pollution Modeling and its Application, Vol. XIV. Proceedings of ITM, Boulder. Plenum Press, New York, pp. 381–389.

Seibert, P., Stohl, A., 2000. Inverse modelling of the ETEX-1 release with a Lagrangian particle model. In: Barone, G., Builtjes, P.J., Giunta, G. (Eds.), GLObal and REgional Atmospheric Modelling. Annali dell'Istituto Universitario Navale di Napoli, Special Issue, 95–105. Proceedings of the Third GLOREAM Workshop, September 1999, Ischia, Italy.

Seibert, P., Kromp-Kolb, H., Baltensperger, U., Jost, D.T., Schwikowski, M., 1994. Trajectory analysis of high-alpine air pollution data. In: Gryning, S.-E., Millan, M.M. (Eds.), Air Pollution Modelling and its Application, Vol. X, Plenum Press, New York, pp. 595–596.

Seibert, P., Krüger, B., Frank, A., 2001. Parametrisation of convective mixing in a Lagrangian particle dispersion model. Proceedings of the Fifth GLOREAM Workshop, Wengen, Switzerland, 24–26 September 2001.

Siems, S.T., Hess, G.D., Suhre, K., Businger, S., Draxler, R., 2000. The impact of wind shear on observed and simulated trajectories during the ACE-1 Lagrangian experiments. Australian Meteorological Magazine 30, 579–587.

Smith, F.B., 1965. The role of windshear in horizontal diffusion of ambient particles. Quarterly Journal of the Royal Meteorological Society 91, 318–329.

Stohl, A., 1996. Trajectory statistics—a new method to establish source–receptor relationships of air pollutants and its application to the transport of particulate sulfate in Europe. Atmospheric Environment 30, 579–587.

Stohl, A., 1998. Computation, accuracy and applications of trajectories—a review and bibliography. Atmospheric Environment 32, 947–966.

Stohl, A., Thomson, D.J., 1999. A density correction for Lagrangian particle dispersion models. Boundary-Layer Meteorology 90, 155–167.

Stohl, A., Trickl, T., 1999. A textbook example of long-range transport: simultaneous observation of ozone maxima of stratospheric and North American origin in the free troposphere over Europe. Journal of the Geophysical Research 104, 30445–30462.

Stohl, A., Wotawa, G., 1995. A method for computing single trajectories representing boundary layer transport. Atmospheric Environment 29, 3235–3239.

Stohl, A., Wotawa, G., Seibert, P., Kromp-Kolb, H., 1995. Interpolation errors in wind fields as a function of spatial and temporal resolution and their impact on different types of kinematic trajectories. Journal of Applied Meteorology 34, 2149–2165.

Stohl, A., Hittenberger, M., Wotawa, G., 1998. Validation of the Lagrangian particle dispersion model FLEXPART against large scale tracer experiment data. Atmospheric Environment 32, 4245–4264.

Thomson, D.J., 1987. Criteria for the selection of stochastic models of particle trajectories in turbulent flows. Journal of Fluid Mechanics 180, 529–556.

Walmsley, J.L., Mailhot, J., 1983. On the numerical accuracy of trajectory models for long-range transport of atmospheric pollutants. Atmospheric Ocean 21, 14–39.